processes

MDPI

Communication

Fabrication of Macroporous Nafion Membrane from Silica Crystal for Ionic Polymer-Metal Composite Actuator

Xiaojun Zhang [1,*], Man Wang [1], Manhong Li [1], Minglu Zhang [1] and Chengwei Zhang [2]

[1] School of Mechanical Engineering, Hebei University of Technology, Tianjin 300130, China; 202011201012@stu.hebut.edu.cn (M.W.); lmh9181219@163.com (M.L.); zhangml@hebut.edu.cn (M.Z.)

[2] School of Materials Science & Engineering and Tianjin Key Laboratory of Materials Laminating Fabrication and Interface Control Technology, Hebei University of Technology, Tianjin 300130, China; cwzhang@hebut.edu.cn

* Correspondence: xjzhang@hebut.edu.cn; Tel.: +86-138-2100-3733

Received: 3 September 2020; Accepted: 28 October 2020; Published: 31 October 2020

Abstract: Nafion membrane with macropores is synthesized from silica crystal and composited with Pt nanoparticles to fabricate macroporous ionic polymer-metal composite (M-IPMC) actuator. M-IPMC shows highly dispersed small Pt nanoparticles on the porous walls of Nafion membrane. After the electromechanical performance test, M-IPMC actuator demonstrates a maximum displacement output of 19.8 mm and a maximum blocking force of 8.1 mN, far better than that of IPMC actuator without macroporous structure (9.6 mm and 2.8 mN) at low voltages (5.8–7.0 V). The good electromechanical performance can be attributed to interconnected macropores that can improve the charge transport during the actuation process and can allow the Pt nanoparticles to firmly adsorb, leading to a good electromechanical property.

Keywords: nafion membrane; ionic polymer-metal composite actuator; macroporous structure; silica crystal; nanoparticles; nanocomposites

1. Introduction

Since Oguro's group investigated bending behavior under an applied electric field for the first time in 1992, ionic polymer-metal composite (IPMC) is considered as a unique electro-active material [1]. Owing to its light weight and large bending deformation under low driving voltage, IPMC has been attracted much attention in smart robot field like artificial muscle [2]. A typical IPMC actuator is composed of an ion-change polymer membrane (e.g., Nafion or Flemion) and metal (Pt or Au), coated on both sides of the polymer, that are used as working electrodes. Under the electric field, the blocking force and displacement are attributed to the migration of cations (normally Li^+) in the channels of the ion-change membrane. The electrochemical performance of IPMC is depending on various actors, such as the size of metal particles [3], types of polymer [4], and the surface structure of the polymer [5]. Based on above actuation mechanism, the structure of the polymer may play an important role in enhancing the electrochemical performance of IPMC because it can greatly affect the transmission of cations. Furthermore, Pt or Au cannot be plated well on the surface of the polymer without surface treatment. To improve the electrochemical properties of IPMC, one of the most commonly used structure modification methods is sandblasting [6]. However, it is difficult to control the morphology of polymer, and it modifies the surface of the polymer and cannot provide more transport channels for cations. Herein, a kind of Nafion membrane with interconnected macroporous structure is prepared from silica crystal as template. After depositing Pt nanoparticles, M-IPMC is produced. The macroporous structure in Nafion membrane is in favor of the formation of the small Pt nanoparticles, increasing the

interface area between Pt and polymer, leading to a good electromechanical property. In addition, the interconnected macropores can provide the fast transport channels of Li ions [7].

2. Materials and Methods

2.1. Materials

Nafion solution (5 wt%) was obtained from DuPont Beijing, China (N,N-dimethyl formamide (DMF, 99.8%) was purchased from Kermel Chemical Co. (Kermel Chemical Co., Tianjin, China); $[Pt(NH_4)_2]Cl_4$ (52 wt%), Lithium hydroxide (LiCl, 98%), Ethanol (C_2H_6O, 99.5%) and methane acid (HCOOH, 88%) was obtained from Shanghai Aladdin Biochemical Technology Co. Hydrochloric acid (HCl, 37%) was purchased from Sigma-Aldrich (Shanghai, China). Hydrofluoric acid (HF, 40%) was obtained from MACKLIN Biochemical Technology Co., LTD (Shanghai, China). The thermostat oven is purchased by Lichen Instrument Technology Co. LTD (LICHEN China 202-00bs 10–250 °C, Shanghai, China).

2.2. Preparation of Macroporous Nafion Membrane

Figure 1 presents the typical preparation process for the macroporous Nafion film. First, monodispersed silica spheres were fabricated by the published method [8–10]. Second, the silica spheres (450 nm in diameter) in ethanol were organized them into close-packed arrays on the glass slide during the evaporation of ethanol at the room temperature for three days. Third, the glass slide was transferred and immersed into the solution containing 14 mL Nafion (5 wt%, DuPont China) and 3.5 mL N, N-dimethylformamide (500 mL, 99.8%). After volatilization of solvent, completely for 24 h at 70 °C in the thermostat oven (Lichen Instrument Technology Co. LTD, Shanghai, China, LICHEN China 202-00bs 10–250 °C), silica/polymer composite was produced. Finally, the macroporous Nafion film was obtained after soaking the silica/polymer composite in 4% HF (AR 40%) solution for 24 h. For comparison, Nafion film without macroporous structure (IPMC) was prepared by the same steps but without the silica crystal.

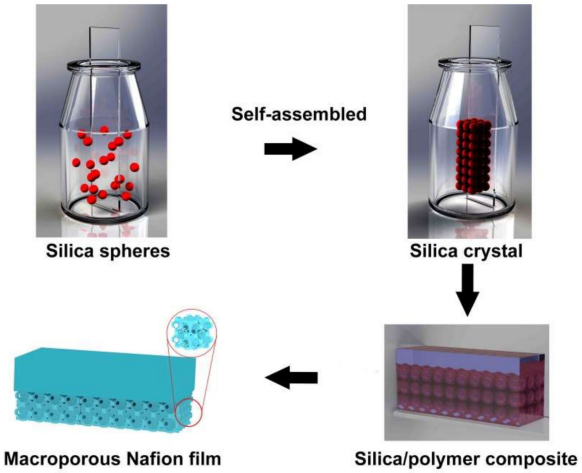

Figure 1. Schematic illustration on the synthesis of Nafion macroporous membrane.

2.3. Preparation of IPMC with Macroprous Structure (M-IPMC)

To deposit the Pt nanoparticles on the surface of Nafion film, the prepared Nafion film was firstly immersed in 20 mL solution with 2 M of $[Pt(NH_4)_2]Cl_4$ (Pt 52%). Then, 10 mL of HCOOH (88%) solution was added in the above solution and stand still for three days. After reduction for 3 days, the film was ultrasonic washed in the DI water and immersed in 20 mL of 2 M LiCl (98%, Shanghai Aladdin Biochemical Technology Co., Shanghai, China) solution at room temperature for 3 days. Finally, M-IPMC was obtained after ionic exchange for 3 days.

2.4. Characterization of M-IPMC

The morphologies of the samples were characterized by field-emission scanning electron microscopy (JEOL Ltd., Akishima, Japan, FESEM, JSM-7100F) at 200 kV. Pt particles were attached to Nafion membrane in the IPMC actuators. And samples were adhesive by conductive tape as the substrate. Before using SEM, the samples were coated with a thin layer of gold, approximately 10 nm. Powder X-ray diffraction analysis was conducted on a Rigaku D/max-2500PC X-ray diffractometer (Rigaku, Tokyo, Japan) with Cu-Kα radiation (λ = 1.5418 Å). The samples were characterized by glass as the substrate. X-ray photoelectron spectroscopy (XPS) analysis was carried out on ESCALAB 250 X-ray photoelectron spectrometer (UZONELAB, Shanghai, China) using Al Kα X-rays as the excitation source. FT-IR spectra were acquired using a VERTEX V80 (BRUKER Ltd., Bremen, German) series spectrometer as transmittance data, with KBr as reference, to certify the presence of oxygen-containing functional groups in Nafion membrane.

Laser displacement sensor was obtained by OPTEX Company Ltd., (Otsu, Japan, CDX85A, 85 ± 20 mm). Force sensor was purchased by MANTON (Osaka, Japan, LRS-20g, 196.1 mN). A signal generator was purchased by UNIT Technology Company (Dongguan, China).

3. Results and Discussion

XRD is applied to further investigate the Pt particle sizes on the Nafion film with or without macropores (Figure 2a). Compared with XRD pattern of Nafion membrane, XRD patterns of M-IPMC and IPMC both exhibit four peaks at 2θ values of about 39.7°, 46.2°, 67.5°, 81.2° and 85.7° which can be ascribed to the (111), (200), (220), (311) and (222) planes of face-centered cubic (fcc) crystalline Pt. However, IPMC demonstrate sharper diffraction peaks than M-IPMC, suggesting that the most of Pt nanoparticles are inserted in the macropores of Nafion membrane. And the crystalline size of Pt on M-IPMC, calculated by using the Scherrer equation from the full width at half maximum (FWHM) of the (220) peak (2θ = 67.5°), is ~2 nm, much smaller than that of IPMC (9 nm) and the reported IPMC actuators [11–14]. XRD results shows Pt nanoparticles of M-IPMC are small resulting in wide FWHM, which has also been reported in many literatures [14] in the Figure 2. The XRD results confirm the effect of the macroporous structure of Nafion membrane, preventing the growth of the Pt nanoparticles [7,15]. Figure 2b shows the FT-IR spectra of the pure Nafion membranes. FT-IR results present Nafion membrane peaks at 1132 and 1203 cm^{-1}, which shows the perfluoroethylen backbone of Nafion film. The characteristic peaks of the side chains in Nafion are showed at 970 cm^{-1}, 1052 cm^{-1}, 1130–1200 cm^{-1}, which were assigned, respectively, to the symmetric vibration of C-O-C bonds and S-O stretching vibration of -SO_3- groups [16,17]. XPS measurement is employed to further characterize the surface chemical states of elements in the prepared IPMC with microporous structure (M-IPMC) (Figure 2c). Figure 2c indicates that XPS spectrum of M-IMPC shows signals of Pt, C, N, O and F elements, demonstrating that Pt nanoparticles have been successfully deposited on Nafion film [16,18,19].

Figure 3a–c show the SEM images of macroporous Nafion film and the uniform macropores over tens of microns length scale can be observed. From Figure 3c, the mean macropore size of Nafion membrane is ca. 400 nm, which is smaller than that of the diameter of original silica spheres (450 nm), owing to the condense of the polymer [8]. Figure 3d–f display the SEM image of M-IPMC after depositing Pt nanoparticles on the surface of Nafion film, demonstrating small and highly dispersed Pt nanoparticles on macroporous Nafion film. In contrast, the Pt nanoparticles tend to aggregation when deposited on the pure Nafion film (Figure 3g–i), indicating that the macroporous structure on the Nafion film plays an important role in controlling the growth and agglomeration of Pt nanoparticles. Under the SEM images of typical IPMC samples, Pt particles show agglomeration, which is due to the smoothness of Nafion membrane surface. From SEM images of typical IPMC samples, agglomerated Pt nanoparticles can be observed, which is due to the smoothness of the Nafion membrane surface. It is well known that support with porous structure would prevent the growth of the Pt nanoparticles,

resulting in dispersed Pt nanoparticles [14]. Also, the size of Pt particles in M-IPMC is smaller than typical IPMC. So, the macroporous structure can inhibit the growth of platinum particles [7,14].

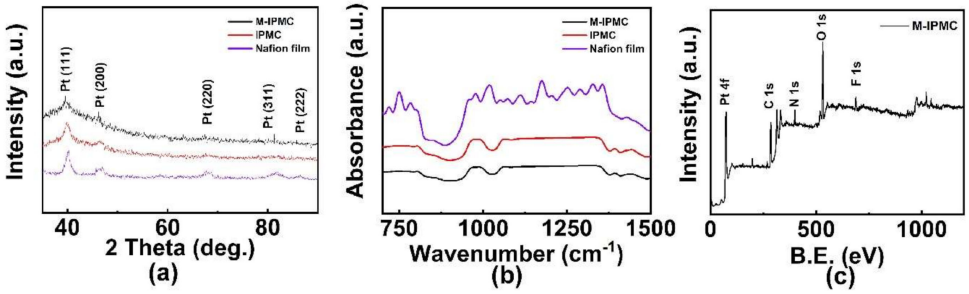

Figure 2. (**a**) XRD patterns of macroporous ionic polymer-metal composite (M-IPMC), IPMC and Nafion film, IPMC and Nafion film, (**b**) FT-IR spectra of M-IPMC IPMC and Nafion film, (**c**) Surface survey XPS spectrum of M-IPMC.

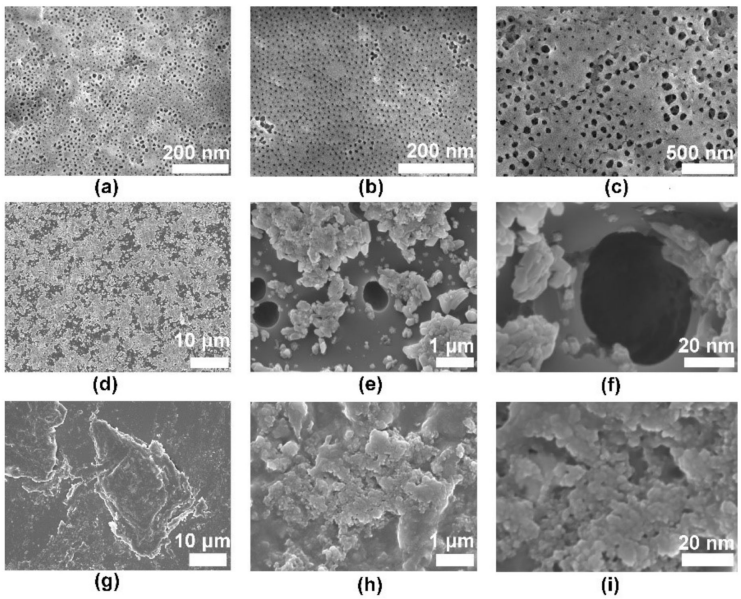

Figure 3. SEM images of (**a**–**c**) macroporous Nafion memebrane, (**d**–**f**) M-IPMC and (**g**–**i**) IPMC actuator.

The electromechanical performances of IPMC actuators have been evaluated by tip displacement and blocking force. The typical blocking force curve and displacement curve are demonstrated in Figure 4a–f. The tip displacement is recorded by a laser displacement sensor (OPTEX Company, CDX85A, 85 ± 20 mm) under ac voltages from 5.8 V to 7.0 V (0.2 Hz). The actuators are cut into a dimension of 40 mm × 10 mm with a thickness of ~0.2 mm [20]. The tip displacement test platform is construed, IPMC is fixed to the clip of the iron rack, and two copper wires are pasted with adhesive tape on both sides of the IPMC [20,21]. The signal generator is connected to the copper wire and the AC voltage of 5.8–7.0 V is loaded, respectively. At room temperature, IPMC was immersed in DI water for 5 min before installing [20,21]. The displacement variation of IPMC was measured by a laser displacement sensor. A high precision force sensor was placed at the tip of IPMC to test the blocking force of IPMC. Both sensors use a PC to collect data. The durability of IPMC is tested by loading different voltages by a signal generator because of IPMC leakage in air, water will gradually be lost and output performance will be gradually reduced [20,21]. Due to the uncertainty of IPMC, the two samples were measured 20 times for each voltage and the highest displacement or force output of five groups (5.8 V, 6.0 V, 6.4 V, 6.8 V and 7.0 V) were calculated the mean as results in Figure 4.

Figure 4a shows the maximum displacement outputs of 19.8 mm under 5.8 V and 15.3 mm under 6.4 V for M-IPMC after 300 s, followed by a fast relaxation that causes an abrupt decay of displacement

after 400 s. The displacement curves of M-IPMC exhibits stable working time of 100 s. In Figure 4b, IPMC actuator shows the stable displacement of 9.6 mm under 6.4 V and 6.5 mm under 7.0 V after 300 s. And there is the sign of relaxation observed in the IMPC actuator after 300 s. This suggests two actuators show different displacement outputs due to the different structure of Nafion film. Figure 4c exhibits a corresponding maximum displacement of two actuators at various voltages, clearly showing the maximum displacement of M-IPMC is much larger than that of IPMC. Furthermore, the maximum displacement is larger than that of the reported IPMCs (10 mm, 14 mm, 3.0 mm) as is shown in Table 1 [22–24].

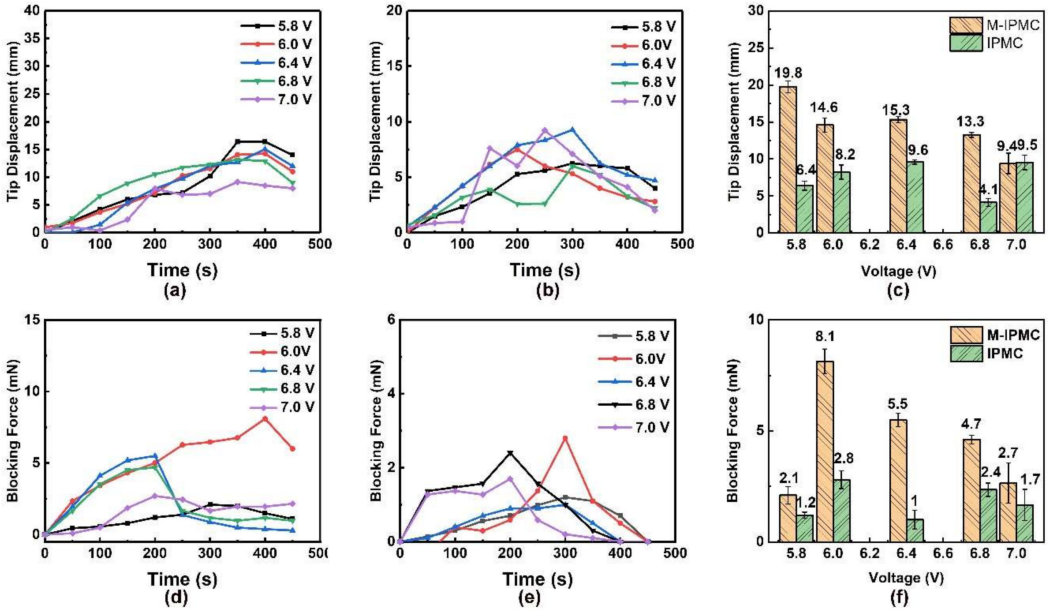

Figure 4. (**a**) Representative tip displacement curves of M-IPMC, (**b**) representative tip displacement curves of IPMC, (**c**) relationship between the maximum displacement and the various voltages (5.8 V–7.0 V), (**d**) representative blocking force curves of M-IPMC, (**e**) representative blocking force curves of IPMC, (**f**) relationship between the maximum blocking force and the various voltages.

Table 1. Comparison mechanical properties of M-IPMC and IPMC.

Samples	Tip Displacement (mm)	Blocking Force (mN)
M-IPMC	19.8	8.1
IPMC	15.3	5.5
[22]	10	5.5
[23]	14	-
[24]	3.0	-
[4]	-	0.64
[5]	-	0.16
[6]	-	4.2

The blocking forces of the prepared samples are tested by a force sensor (LRS-20g, 196.1 mN, MANTON). As shown in Figure 4d, the stable blocking force of M-IPMC is 8.1 mN under 6.0 V after 400 s and 5.5 mN under 6.4 V after 200 s, followed by a fast relaxation that causes an abrupt decay in the blocking force after 400 s and 200 s, respectively. For IPMC, in Figure 4e, the stable blocking force is 2.8 mN under 6.0 V after 300 s and 2.4 mN under 6.4 V after 250 s. Also, there is a sign of abrupt decay after 300 s under 6.0 V and 250 s under 6.4 V, respectively. This finding indicates that the response time of M-IPMC is faster than that of IPMC, which can be attributed to the smaller Pt nanoparticles and slower water loss caused by macroporous structure [25,26]. As is shown in Figure 4f, the maximum force of M-IPMC actuator is far larger than that of the IPMC actuator. Also, the maximum blocking

force of the M-IPMC actuator is higher than that of the reported actuator (0.64 mN, 1.6 mN and 4.2 mN) as is shown in Table 1 [4–6]. Since the peak blocking force of M-IPMC is decayed as voltages decreased, the blocking force of actuators can be controlled under certain low voltages (5.8–6.0 V). The superior mechanical performance of M-IPMC is attributed to the macroporous structure that can improve the rapid transportation of Li ions and highly dispersed small Pt nanoparticles that can enhance water-saving capacity of IPMC actuators and conductivity [7].

4. Conclusions

Nafion film with macroporous structure has been successfully prepared by using silica crystal as a template. After depositing Pt nanoparticles on the macroporous Nafion membrane and Li+ exchanging, M-IPMC was formed. The M-IPMC actuators exhibit enhanced electromechanical performance (the maximum displacement output is 19.8 mm and the maximum blocking force is 8.1 mN) compared with typical IPMC actuator. The good electromechanical properties of M-IPMC can be ascribed to the macroporous structure in Nafion membrane that is in favor of the improvement of the interface area between Pt and polymer, leading to a good electromechanical property and can provide the fast transport channels of Li ions.

Author Contributions: X.Z. and M.W. conducted the experiments. M.L. and M.Z. performed data analyses. M.W. and C.Z. contributed to the writing of the manuscript. All authors have read and agreed to the published version of the manuscript.

Funding: This work was supported by the National Natural Science Foundation of China (Grant No. 61803142) and the National Natural Science Foundation of Hebei Province (Grant No. F2018202210).

Conflicts of Interest: The authors declare no conflict of interest.

References

1. Oguro, K.; Kawami, Y.; Takenaka, H. Bending of an ion-conducting polymer film-electrode composite by an electric stimulus at low voltage. *J. Micromach. Soc.* **1992**, *5*, 27–30.
2. Zhao, G.; Sun, Z.; Guo, H.; Zheng, J.; Wang, H.; Wang, Z. Combination mechanism investigation on the muscle-like linear actuator using ionic polymer metal composites. *Polym. Compos.* **2015**, *38*, 479–488. [CrossRef]
3. Wang, J.; Wang, Y.; Zhu, Z.; Wang, J.; He, Q.; Luo, M. The Effects of Dimensions on the Deformation Sensing Performance of Ionic Polymer-Metal Composites. *Sensors* **2019**, *19*, 2104. [CrossRef] [PubMed]
4. Khan, A.; Jain, R.K.; Luqman, M.; Asiri, A.M. Development of sulfonated poly(vinyl alcohol)/aluminium oxide/graphene based ionic polymer-metal composite (IPMC) actuator. *Sens. Actuator A Phys.* **2018**, *280*, 114–124. [CrossRef]
5. Saccardo, M.C.; Zuquello, A.G.; Tozzi, K.A.; Gonçalves, R.; Hirano, L.A.; Scuracchio, C.H. Counter-ion and humidity effects on electromechanical properties of Nafion®/Pt composites. *Mater. Chem. Phys.* **2020**, *244*, 122674. [CrossRef]
6. Jung, S.Y.; Park, J.-O.; Park, S. Replacement of surface roughening using polyvinyl alcohol coating in the fabrication of nafion-based ionic polymer metal composite (IPMC) actuators. *J. Polym. Res.* **2016**, *23*, 1–6. [CrossRef]
7. Guo, D.-J.; Fu, S.-J.; Tan, W.; Dai, Z.-D. A highly porous nafion membrane templated from polyoxometalates-based supramolecule composite for ion-exchange polymer-metal composite actuator. *J. Mater. Chem.* **2010**, *20*, 10159–10168. [CrossRef]
8. Guo, Z.; Wang, F.; Xia, Y.; Li, J.; Tamirat, A.G.; Liu, Y.; Wang, L.; Wang, Y.; Xia, Y.-Y. In situ encapsulation of core–shell-structured Co@Co3O4 into nitrogen-doped carbon polyhedra as a bifunctional catalyst for rechargeable Zn–air batteries. *J. Mater. Chem. A* **2018**, *6*, 1443–1453. [CrossRef]
9. Yu, Q.; Nie, Y.; Cui, Y.; Zhang, J.; Jiang, F. Single-ion Polyelectrolyte/ Mesoporous Hollow-Silica Spheres, Composite Electrolyte Membranes for Lithium-ion Batteries. *Electrochimica Acta* **2015**, *182*, 297–304. [CrossRef]
10. Zhang, Y.; Xue, R.; Zhong, Y.; Jiang, F.; Hu, M.; Yu, Q. Nafion/IL Intermediate Temperature Proton Exchange Membranes Improved by Mesoporous Hollow Silica Spheres. *Fuel Cells* **2018**, *18*, 389–396. [CrossRef]
11. He, Q.; Yu, M.; Yu, D.; Ding, Y.; Dai, Z. Significantly Enhanced Actuation Performance of IPMC by Surfactant-Assisted Processable MWCNT/Nafion Composite. *J. Bionic Eng.* **2013**, *10*, 359–367. [CrossRef]

12. Tas, S.; Zoetebier, B.; Sukas, O.S.; Bayraktar, M.; Hempenius, M.A.; Vancso, G.J.; Nijmeijer, D.C. Ion-Selective Ionic Polymer Metal Composite (IPMC) Actuator Based on Crown Ether Containing Sulfonated Poly(Arylene Ether Ketone). *Macromol. Mater. Eng.* **2016**, *302*, 1600381. [CrossRef]
13. Tripathi, A.S.; Chattopadhyay, B.P.; Das, S. Cost-effective fabrication of ionic polymer based artificial muscles for catheter-guidewire maneuvering application. *Microsyst. Technol.* **2018**, *25*, 1129–1136. [CrossRef]
14. Zhang, C.; Xu, L.; Shan, N.; Sun, T.; Chen, J.; Yan, Y. Enhanced Electrocatalytic Activity and Durability of Pt Particles Supported on Ordered Mesoporous Carbon Spheres. *ACS Catal.* **2014**, *4*, 1926–1930. [CrossRef]
15. Mehraeen, S.; Sadeghi, S.; Cebeci, F.Ç.; Papila, M.; Gürsel, S.A. Polyvinylidene fluoride grafted poly(styrene sulfonic acid) as ionic polymer-metal composite actuator. *Sens. Actuator A Phys.* **2018**, *279*, 157–167. [CrossRef]
16. Li, Y.; Intikhab, S.; Malkani, A.; Xu, B.; Snyder, J.D. Ionic Liquid Additives for the Mitigation of Nafion Specific Adsorption on Platinum. *ACS Catal.* **2020**, *10*, 7691–7698. [CrossRef]
17. Naji, L.; Chudek, J.A.; Abel, E.W.; Baker, R.T. Electromechanical behaviour of Nafion-based soft actuators. *J. Mater. Chem. B* **2013**, *1*, 2502–2514. [CrossRef]
18. Kalyva, M.; Sunding, M.F.; Gunnæs, A.E.; Diplas, S.; Redekop, E.A. Correlation between surface chemistry and morphology of PtCu and Pt nanoparticles during oxidation-reduction cycle. *Appl. Surf. Sci.* **2020**, *532*, 147369. [CrossRef]
19. Yaqoob, L.; Noor, T.; Iqbal, N.; Nasir, H.; Zaman, N.; Talha, K. Electrochemical synergies of Fe–Ni bimetallic MOF CNTs catalyst for OER in water splitting. *J. Alloys Compd.* **2021**, *850*, 156583. [CrossRef]
20. He, Q.; Yu, M.; Ding, Y.; Dai, Z.-D. Fabrication and characteristics of a multilayered ionic polymer metal composite based on Nafion/tetraethyl orthosilicate and Nafion/MCNT nanocomposites. *J. Nanosci. Nanotechnol.* **2014**, *14*, 7445–7450. [CrossRef]
21. Wisniewski, H.; Plonecki, L. The dynamic properties of the IPMC polymer. In Proceedings of the 2015 16th International Carpathian Control Conference (ICCC), Szilvasvarad, Hungary, 27–30 May 2015; pp. 594–598.
22. Yip, J.; Ding, F.; Yick, K.L.; Yuen, C.-W.M.; Lee, T.-T.; Choy, W.-H. Tunable carbon nanotube ionic polymer actuators that are operable in dry conditions. *Sens. Actuators B Chem.* **2012**, *162*, 76–81. [CrossRef]
23. Jain, R.; Datta, S.; Majumder, S.; Mukherjee, S.; Sadhu, D.; Samanta, S.; Banerjee, K. Bio-mimetic Behaviour of IPMC Artificial Muscle Using EMG Signal. In Proceedings of the 2010 International Conference on Advances in Recent Technologies in Communication and Computing, Kottayam, India, 16–17 October 2010; pp. 186–190.
24. Wei, H.-C.; Su, G.-D.J. A large-stroke deformable mirror by gear shaped IPMC design. In Proceedings of the 2011 6th IEEE International Conference on Nano/Micro Engineered and Molecular Systems, Kaohsiung, Taiwan, 20–23 February 2011; pp. 113–116.
25. Lian, H.; Qian, W.; Estevez, L.; Liu, H.; Liu, Y.; Jiang, T.; Wang, K.; Guo, W.; Giannelis, E.P. Enhanced actuation in functionalized carbon nanotube–Nafion composites. *Sens. Actuators B Chem.* **2011**, *156*, 187–193. [CrossRef]
26. Nguyen, V.K.; Lee, J.-W.; Yoo, Y. Characteristics and performance of ionic polymer-metal composite actuators based on Nafion/layered silicate and Nafion/silica nanocomposites. *Sens. Actuators B Chem.* **2007**, *120*, 529–537. [CrossRef]